Radiolabeled, Nonspecific, Polyclonal Human Immunoglobulin in the Detection of Focal Inflammation by Scintigraphy: Comparison with Gallium-67 Citrate and Technetium-99m-Labeled Albumin

Robert H. Rubin, Alan J. Fischman, Mark Needleman, Robert Wilkinson, Ronald J. Callahan, Ban-An Khaw, W. Peter Hansen, Peter B. Kramer, and H. William Strauss

Infectious Disease Unit of the Medical Service and the Division of Nuclear Medicine of the Department of Radiology of the Massachusetts General Hospital, Departments of Medicine and Radiology, Harvard Medical School, Boston, MA, The Cambridge Research Laboratory, Cambridge, MA and Ortho Biotech Imaging Products, Washington Crossing, New Jersey

The accumulation of nonspecific polyclonal human immunoglobulin (IgG) radiolabeled with ^{125}I or ^{111}In was compared to that of [^{67}Ga]citrate and [^{99m}Tc]albumin in rats with deep thigh inflammation due to *Escherichia coli* infection. Serial scintigrams were acquired at 1, 3, 24, and in some cases, 48 hr after injection. As early as 3 hr postinjection, [^{111}In]IgG showed greater accumulation at the lesion than [^{99m}Tc]HSA ($p < 0.01$). Both [^{125}I]IgG and [^{111}In]IgG showed greater accumulation than [^{67}Ga]citrate ($p < 0.01$). At 24 hr, IgG image definition increased, while HSA image definition decreased, and the intensity of accumulation of both IgG preparations was greater than that of [^{67}Ga]citrate or [^{99m}Tc]HSA ($p < 0.01$). At all imaging times, [^{67}Ga]citrate accumulation was surprisingly low. In inflammation produced by *Pseudomonas aeruginosa*, *Staphylococcus aureus*, *Klebsiella pneumoniae*, *Candida albicans*, or turpentine, [^{111}In]IgG accumulation was similar to the results obtained with *Escherichia coli*. These studies suggest that focal sites of inflammation can be detected with radiolabeled nonspecific human polyclonal IgG.

J Nucl Med 30:385–389, 1989

An integral part of the evaluation of febrile patients is the prompt identification of focal sites of infection. In many instances, demonstration of the anatomic site of the process is more important than identifying the microbial content of the abscess (*1*). While conventional radiography, computed tomography (CT), or ultrasonic scanning (US) can localize these lesions in most patients, these anatomic techniques usually require formation of an abscess before definitive radiographic findings are present. Radionuclide imaging with gallium-67 (^{67}Ga)citrate or labeled leukocytes can usually detect lesions of infectious etiology prior to formation of an abscess, but typically require 24 hr between injection and imaging to detect sites of inflammation. This interval may be too long for managing acutely ill patients with multisystem disease.

In the course of studies of deep soft-tissue *Pseudomonas aeruginosa* infections in a rat model, two potential new approaches for detecting focal infections were suggested (*2*). First, specific immune imaging of an infectious process using a monoclonal antibody specific for a unique microbial antigen, in this case the *Pseudomonas* Type I specific polysaccharide, was shown to be possible. In addition, a second approach appeared possible: nonspecific radiolabeled IgG localized at the lesion site to an extent sufficient to provide clear delineation of the process. This raised the possibility that a generic inflammation scan may be practical, based on

Received June 13, 1988; revision accepted Oct. 12, 1988.

For reprints contact: Robert H. Rubin, MD, Infectious Disease Unit, Massachusetts General Hospital, Boston, MA 02114.

the accumulation of nonspecific IgG at the site. This report documents the feasibility of the nonspecific approach, comparing the localization of radiolabeled IgG, [^{67}Ga]citrate and [^{99m}Tc]albumin at sites of acute inflammation in a rat model.

MATERIALS AND METHODS

Radiopharmaceuticals

Human, nonspecific, polyclonal immunoglobulin (Sandoglobulin, Sandoz, Inc., East Hanover, NJ) modified for intravenous use (*1*) was radiolabeled with either iodine-125 (^{125}I) or indium-111 (^{111}In) (Amersham, Arlington Heights, IL). Radioiodinated antibodies were prepared by the iodogen method (*3*). Antibodies were radiolabeled with ^{111}In (*1*) via the diethylenetriaminepentaacetic acid (DTPA) antibody chelate method as originally described by Krecjarek and Tucker (*4*) and modified by Khaw et al. (*5*). After labeling, the immunoglobulin preparations were chromatographed on a Sephadex G-25 column to remove unbound radiolabel.

In some experiments, either or both [^{67}Ga]citrate (DuPont Company, No. Billerica, MA) (*1*) and technetium-99m-(^{99m}Tc) labeled human serum albumin (Medi-Physics, Richmond, CA) (*1*) were co-injected with radiolabeled IgG.

Overview of Experiments

Groups of rats (Charles River Breeding Laboratories, Burlington, MA) with focal inflammation in the thigh were imaged following injection of: (a) IgG alone; (b) IgG and [^{67}Ga] citrate; and (c) IgG, [^{67}Ga]citrate and [^{99m}Tc]HSA.

These experiments were performed both to confirm the utility of nonspecific IgG for localizing focal sites of inflammation and to compare two different nonspecific methods, i.e., [^{67}Ga]citrate and [^{99m}Tc]HSA to the immunoglobulin approach for the detection of acute bacterial infection.

Phantom Studies

To determine if data recorded from animals injected simultaneously with more than one radionuclide required correction for crossover of activity from one tracer to the window of the others, sources of ^{99m}Tc, ^{111}In, ^{67}Ga, and ^{125}I were placed in petri dishes (2 × 10 cm) and imaged in all windows. The amount of activity in each dish was approximately equal to the amount proposed for the animal experiments. The sources were imaged with a medium-energy collimator, using centerline and window settings described below. The results were expressed as percent crossover into each window. Phantom imaging was performed immediately after preparation of the sources and 24 hr later (to simulate the conditions of the animal studies).

Animal Model

Single clinical isolates of *Escherichia coli*, *Pseudomonas aeruginosa*, *Staphylococcus aureus*, *Candida albicans*, or *Klebsiella pneumoniae* were employed. The appropriate microbial strain was incubated overnight on trypticase soy agar plates at 37°C. Individual colonies were diluted with sterile normal saline to produce a turbid suspension containing ~2 × 10^9 organisms/ml.

Male Sprague-Dawley rats, weighing ~150 g (*1*) were anesthetized with ether and the lateral aspect of one of their thighs traumatized by pinching with a hemostat. Then 0.1 ml of a suspension containing ~2 × 10^8 organisms (0.1 ml of the turbid suspension in 50% autologous blood/normal saline) was injected into the traumatized thigh muscle. In an additional group of animals, sterile inflammation was created by injection of 0.1 ml of turpentine instead of bacteria. Twenty-four hours later, when gross swelling was apparent in the infected thigh, the radiolabeled reagents were injected intravenously via the tail vein. The animals were reanesthetized with ether and imaged at 1, 3, 24, and 48 hr following injection of the radiopharmaceuticals as described below. At the conclusion of imaging, the anesthetized animals were killed and the infected thigh examined and recultured.

Radiopharmaceutical Dose

IgG: 50 μg (0.25 mg/kg) of IgG labeled with 100–150 μCi of either ^{111}In or ^{125}I; [^{67}Ga]citrate: 200–300 μCi of ^{67}Ga; and [^{99m}Tc]albumin: 300–500 μCi of ^{99m}Tc. Experiments in which IgG, [^{67}Ga] and [^{99m}Tc]HSA co-injected were performed with a fixed ratio of radiolabeled-IgG: ^{67}Ga: ^{99m}Tc of 1:2:4.

Imaging

Following injection of the appropriate radiopharmaceutical(s), the anesthetized animals were placed prone on the medium-energy, parallel hole collimator of a standard field-of-view scintillation camera (Ohio Nuclear 100, Solon, OH). Images were recorded for a preset time of 10 min at the following windows (depending on the nuclide): ^{125}I: 30 keV with a 20% window; ^{67}Ga: 90 keV with a 20% window; ^{99m}Tc: 140 keV with a 20% window; and ^{111}In: 247 keV with a 20% window.

Crossover ratios were determined by imaging pure sources at each window. The crossover values are summarized in Table 1.

Data Analysis

The images were analyzed by placing a region of interest over the infected thigh (target), over a comparable zone of the contralateral thigh (background), and over the entire animal (total residual activity). All data were corrected for crossover prior to calculation. Two values were calculated from this data: (1) The figure of merit [FOM = (target-background)/background]; and (2) the percent residual activity/lesion (PRA). The PRA was calculated by correcting the lesion region of interest counts for background activity (contralateral thigh), to provide the "net counts" in the lesion. The "net counts"

TABLE 1
Percent Crossover

	Radionuclide window			
	^{99m}Tc	^{111}In	^{67}Ga	^{125}I
^{99m}Tc 0 hr*	—	0.4	9.0	0.5
24 hr	—	0.1	4.3	0.0
^{111}In 0 hr	16.4	—	5.2	22.7
24 hr	16.5	—	5.6	24.2
^{67}Ga 0 hr	7.3	6.2	—	1.9
24 hr	8.0	6.1	—	2.0
^{125}I 0 hr	0.0	0.0	0.0	—
24 hr	0.0	0.0	0.0	—

* Measurements were performed immediately after preparation of the sources and 24 hr later.

were divided by the residual total body activity for that radiopharmaceutical to give the percent residual activity/lesion. The formula used to calculate this data is shown below:

$$\% \text{ Residual activity} = \frac{\text{TLC-(BKG*NPL)}}{\text{TBC}}$$

where

TLC = total lesion counts;
BKG = background cts/number of pixels in background;
NPL = number of pixels in lesion; and
TBC = counts in the total body of the animal

Statistical Methods

The relationship of figure of merit [(target-background)/background] and % residual activity for each radiopharmaceutical was compared at each time point by analysis of variance followed by Duncans new multiple range test (*6*). The results are presented as mean ± s.e.m. unless indicated otherwise.

RESULTS

Phantom Studies

The results of these studies are summarized in Table 1. Both ^{111}In and ^{67}Ga caused significant crossover in all the other windows. In contrast, the ^{99m}Tc source had a significant amount of crossover in the ^{67}Ga window and much lower amounts in the other windows. The ^{125}I source did not show significant crossover in any of the other windows. With the ^{99m}Tc source, significantly less crossover into the ^{67}Ga window was detected 24 hr after preparation of the source.

Infection Experiments

A total of 164 animals were studied in 24 separate experiments. In the rat model of deep thigh *Escherichia coli* (96 animals) infection, focal localization of radiolabeled immunoglobulin ([^{125}I]IgG and [^{111}In]IgG) was seen as early as 3 hr postinjection, with the target-to-background ratio of the image continuing to increase until 24 hr after injection (Fig. 1). With other types of bacteria including *Klebsiella pneumonia* (six animals), *Pseudomonas aeruginosa* (24 animals), or; a yeast, *Candida albicans* (ten animals); or the chemical irritant turpentine (15 animals), similar results were obtained 24 hr after injection of [^{111}In]IgG (Fig. 2). Nearly identical results were obtained with *Staphylococcus aureus* infections (15 animals, not shown).

The animals with *E. coli* deep thigh infections that were simultaneously injected with ^{111}In- or ^{125}I-labeled immunoglobulin, [^{67}Ga]citrate, and ^{99m}Tc-labeled HSA provide an excellent model for comparing the imaging properties of the different agents. Serial scintigrams of each isotope acquired at 1, 3, 24, and in some cases, 48 hr after injection revealed the following (Figs. 3 and 4): Figure 3 shows the FOM ratio of deep thigh infections after injection of [^{67}Ga]citrate, [^{99m}Tc]HSA, [^{125}I] IgG and [^{111}In]IgG. Analysis of variance demonstrated a significant main effect of protein preparation; $F_{3,143}$ = 63.81, $p < 0.0001$ and time after injection; $F_{3,143}$ = 2.69, $p < 0.05$. At the various imaging times, the following general pattern of FOM ratio was observed: [^{111}In]IgG > [^{125}I]IgG > [^{99m}Tc]HSA > [^{67}Ga]citrate. At 3 hr, the FOM ratio for [^{111}In]IgG was significantly greater than for [^{125}I]IgG ($p < 0.05$), [^{99m}Tc]HSA ($p < 0.01$) and ^{67}Ga ($p < 0.01$); and the ratio for [^{125}I]IgG was significantly greater than for ^{67}Ga ($p < 0.05$). At 24 hr, the FOM ratios for both IgG preparations was significantly greater ($p < 0.01$) than for [^{67}Ga] or [^{99m}Tc] HSA. At 48 hr the FOM ratio for [^{111}In]IgG was significantly greater than for ^{67}Ga ($p < 0.01$). At 1 hr, a similar trend was detected, but the differences were not statistically significant.

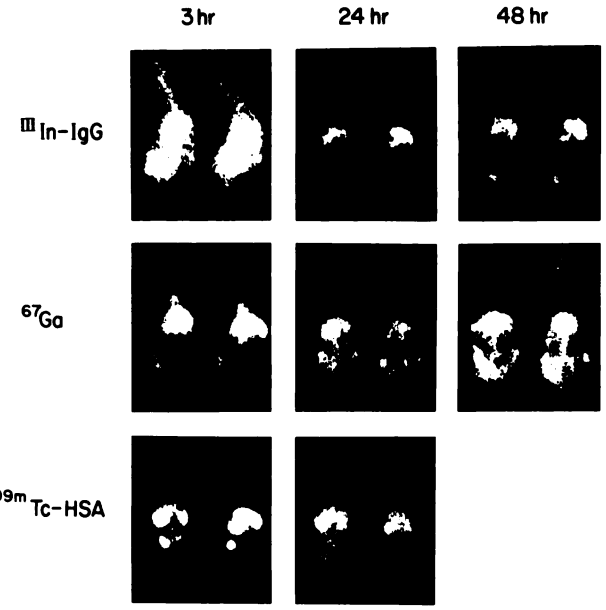

FIGURE 1
Gamma camera images of rats with *E. coli* deep thigh infections imaged at 3, 24, and 48 hr after injection of [^{111}In]IgG, [^{67}Ga]citrate or [^{99m}Tc]HSA. These images represent a subset of the data presented in Figure 3.

For the radiolabeled immunoglobulin preparations, the maximum FOM ratio was detected at 24 hr after injection, while for ^{67}Ga and [^{99m}Tc]HSA, the maximum ratio occurred at 3 hr. The FOM ratio for indium labeled IgG at 24 hr was significantly greater than at all other times; 3 hr ($p < 0.05$), 48 hr ($p < 0.01$); and, the ratio at 3 hr was significantly greater than 48 hr ($p < 0.05$). For [^{125}I]IgG, the ratio at 24 hr was significantly greater than at 1 hr ($p < 0.01$). For [^{99m}Tc]HSA, the ratio was significantly greater at 1 hr ($p < 0.05$) and 3 hr ($p < 0.01$) than at 24 hr. For ^{67}Ga, a significant effect of time on FOM ratio was not detected.

When the data were evaluated as PRA, the difference in behavior of these agents was more striking. Figure 4 shows the percent residual activity of deep thigh infections after injection of [^{67}Ga]citrate, [^{99m}Tc]HSA, [^{125}I] IgG and [^{111}In]IgG. Analysis of variance demonstrated

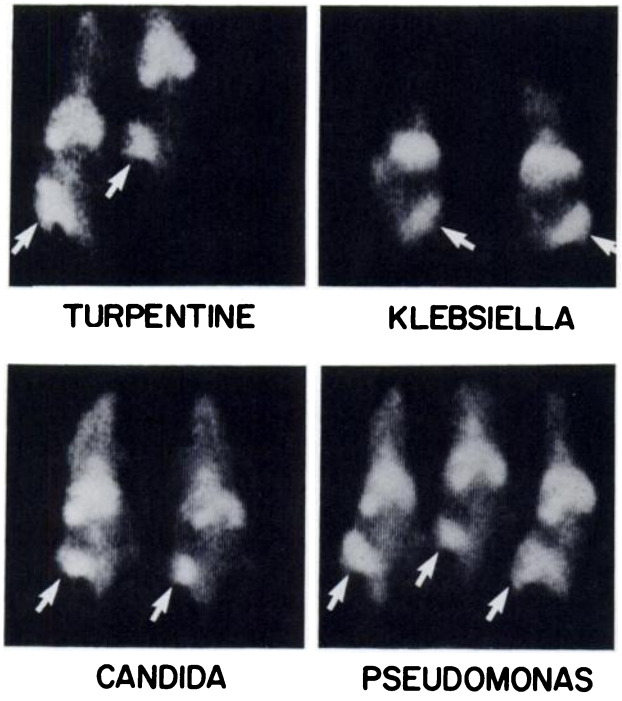

FIGURE 2
Gamma camera images of rats with deep thigh inflammation produced by turpentine (upper left), *Klebsiella pneumonia* (upper right), *Candida albicans* (lower left) and *Pseudomonas aeruginosa* (lower right), images 24 hr after injection of [^{111}In]IgG. Similar results were obtained with *Staphlococcus aureus* infections. Arrows indicate the area of infection.

significant main effects of protein preparation; $F_{3,143}$ = 30.92, $p < 0.0001$ and time after injection; $F_{3,143}$ = 6.26, $p < 0.001$. At 3, 24, and 48 hr, PRA for [^{125}I]IgG was significantly greater ($p < 0.01$) than for the other agents. The PRA for [^{111}In]IgG was greater ($p < 0.01$) than ^{67}Ga (24 and 48 hr) and [^{99m}Tc]HSA (24 hr). At 1 hr, a similar general trend was detected, but the differences were not statistically significant. With the radiolabeled immunoglobulin preparations, maximal PRA was detected at 24 hr. For [^{125}I]IgG, PRA at 24 hr was significantly greater ($p < 0.01$) than at 1 or 3 hr. With [^{111}In]IgG, PRA at 24 hr was greater ($p < 0.05$) than at 3 hr. PRA for ^{67}Ga at 48 hr was greater ($p < 0.05$) than at 1 or 3 hr. For [^{99m}Tc]HSA, a significant effect of time on PRA was not detected.

DISCUSSION

Radiolabeled human polyclonal IgG reliably accumulates at focal sites of inflammation to an extent sufficient to permit imaging of the inflammatory process. The nonspecificity of this agent, and the possibility that it could be clinically useful as a generic inflammation scan, are suggested by two types of observations. First, a wide variety of inflammatory processes, ranging from infections as a result of both gram negative and gram positive bacteria as well as an infection due to a yeast or a nonmicrobial chemical irritant were imaged equally well. It is highly unlikely that this IgG preparation would contain sufficient specific antibody to each of these agents to produce specific images. Rather, it seems reasonable to suggest that the images obtained with labeled IgG are due to nonspecific accumulation at the inflammatory sites.

Inflammation is a stereotyped set of complicated functional and cellular adjustments involving the microcirculation, fluid shifts, and inflammatory cells. The experiments in which animals with focal infection were simultaneously injected with ^{125}I- or ^{111}In-labeled IgG, [^{99m}Tc]HSA, and [^{67}Ga]citrate offer considerable insight into these events. One hour after injection of these agents, the nonspecific leak of serum proteins as a result of increased vascular permeability of the capillary bed at the site of inflammation is identified by exudation of HSA, globulins, and the proteins to which gallium is bound (*7–11*). Previous studies have used the leak of

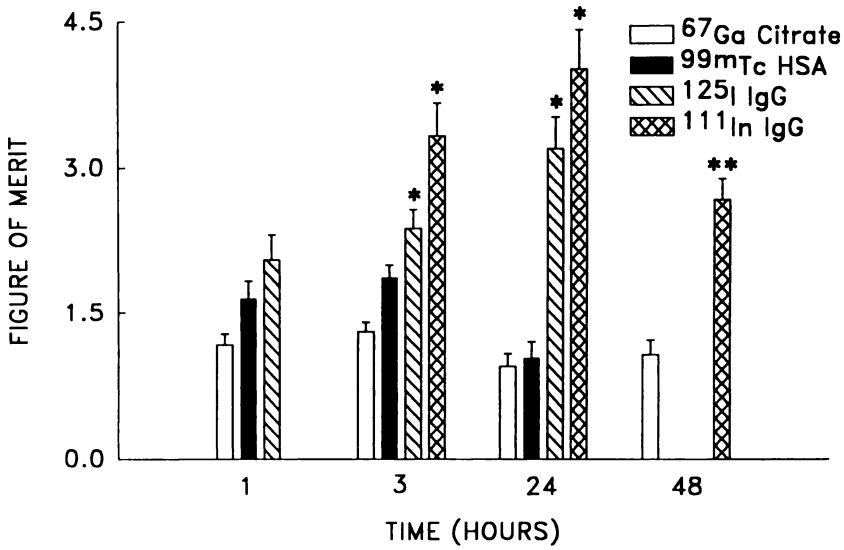

FIGURE 3
Figure of merit (see Methods) for rats with *E. coli* deep thigh infections imaged at 3, 24, and 48 hr after injection of [^{111}In]IgG, [^{67}Ga]citrate or [^{99m}Tc]HSA. All images were corrected for crossover prior to calculation of FOM; *$p < 0.05$, **$p < 0.01$.

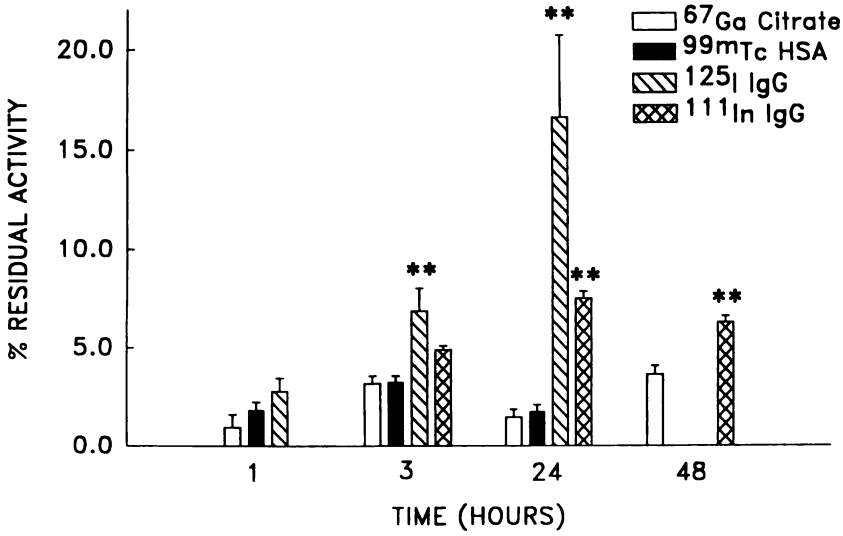

FIGURE 4
Percent residual activity (see Methods) for rats with *E. coli* deep thigh infections imaged at 3, 24, and 48 hr after injection of [^{111}In]IgG, [^{67}Ga]citrate or [^{99m}Tc]HSA. All images were corrected for crossover prior to calculation of PRA; $^{**}p < 0.01$.

either small molecules or proteins as an indication of the degree of injury in tissue (*12,13*). However, following this initial exudation of serum proteins, one of two events occurs. In the case of albumin, for which there are no receptors at the site of inflammation, egress from the inflammatory site, presumably by way of local lymphatic drainage, occurs as easily as ingress into the site. Evidence for this phenomenon comes from the initial increase in activity with relatively rapid loss. In contrast, ^{67}Ga activity at the lesion persists, suggesting some binding at the site of inflammation. However, the degree of ^{67}Ga localization is modest compared to that of IgG. Since all of the experiments were performed with multiple tracers, it is possible that the apparent low level of ^{67}Ga accumulation is due to greater crossover of ^{67}Ga photons into the other windows compared to crossover of non-^{67}Ga photons into the ^{67}Ga window. The crossover studies, summarized in Table 1, indicate this is not the case. In fact, since only the 90 keV photopeak of ^{67}Ga was imaged, crossover was greatest into the ^{67}Ga window (except for Cd x-rays of ^{111}In in the ^{125}I window) and may have falsely elevated the apparent ^{67}Ga uptake. The relative concentration of radiolabeled IgG, expressed either as the FOM (important from the perspective of lesion detection in images) or PRA (important from the perspective of overall count rate at the lesion site) is far higher than that of either [^{99m}Tc]HSA or [^{67}Ga]citrate. It would seem reasonable to hypothesize that at least part of the retention of IgG at the inflammatory site could occur via Fc receptors on inflammatory cells.

These results suggest that an inflammation scan based on nonspecific IgG accumulation is possible. Polyclonal human IgG, modified for intravenous use, was selected for these trials with a view towards early application to imaging of human subjects with focal inflammation.

REFERENCES

1. Ahrenholz OH, Simmons RL. Pancreatitis and other intraabdominal infections. In: Howard RJ, Simmons RL, eds. *Surgical infectious diseases.* Second Ed. Norwalk, CT: Appleton and Lange, 1988: 605–646.
2. Rubin RH, Young LS, Hansen WP, et al. Specific and non-specific imaging of localized Fisher Immunotype I *Pseudomonas Aeruginosa* infection with radiolabeled monoclonal antibody. *J Nucl Med* 1988; 29:651–656.
3. Markwell MA. A new solid state reagent to iodinate proteins. *Anal Biochem* 1982; 125:427–432.
4. Krejcarek GE, Tucker KL. Covalent attachment of chelating groups to macromolecules. *Biochem Biophys Res Commun* 1977; 77:581–585.
5. Khaw BA, Mattis JA, Melincofff G, Strauss HW, Gold HK, Haber E. Monoclonal antibody to cardiac myosin: imaging of experimental myocardial infarction. *Hybridoma* 1984; 3:11–23.
6. Duncan DB. Multiple range tests and multiple F-tests. *Biometrics* 1955; 11:1–42.
7. Chen DC, Newman NJ, Larson SM. Transferrin receptors and gallium-67 uptake in vitro. *Eur J Nucl Med* 1982; 7:536–540.
8. Rasey JS, Nelson NJ, Larson SM. Relationship of iron metabolism to tumor cell toxicity of stable gallium salts. *Int J Nucl Med Biol* 1981; 8:303–313.
9. Tzen KY, Oster ZH, Wagner HN, Tsan MF. Role of iron-binding proteins and enhanced capillary permeability on the accumulation of gallium-67. *J Nucl Med* 1980; 21:31–35.
10. Larson SM, Rasey JS, Allen DR, Nelson NJ. A transferrin-mediated uptake of gallium-67 by ENT-6 sarcoma. I. Studies in tissue culture. *J Nucl Med* 1979; 20:837–842.
11. Tsan MF. Studies on gallium accumulation in inflammatory lesions: III. Roles of polymorphonuclear leukocytes and bacteria. *J Nucl Med* 1978; 19:492–495.
12. Lull RJ, Tatum JL, Sugarman HJ, Hartshorne MF, Boll DA, Kaplan KA. Radionuclide evaluation of lung trauma. *Semin Nucl Med* 1983; 13:223–237.
13. Kadir S, Strauss HW. Evaluation of inflammatory bowel disease with ^{99m}Tc-DTPA. *Radiology* 1977; 130;443–446.